MOLECULAR AND CELLULAR BIOLOGY, Apr. 1995, p. 2145–2156 Vol. 15, No. 4
0270-7306/95/$04.00+0

Turnover Mechanisms of the Stable Yeast *PGK1* mRNA

DENISE MUHLRAD, CAROLYN J. DECKER, AND ROY PARKER*

Department of Molecular and Cellular Biology, Howard Hughes Medical Institute, University of Arizona, Tucson, Arizona 85721

Received 30 September 1994/Returned for modification 10 November 1994/Accepted 13 January 1995

The first step in the decay of several yeast mRNAs is the shortening of the poly(A) tail, which for the *MFA2* transcript triggers decapping and 5′-to-3′ degradation. To understand the basis for differences in mRNA decay rates, it is important to determine if deadenylation-dependent decapping is specific to the unstable *MFA2* transcript or is a general mechanism of mRNA degradation. To this end, we analyzed the turnover of the stable *PGK1* mRNA by monitoring the decay of a pulse of newly synthesized transcripts while using two strategies to trap decay intermediates. First, we used strains deleted for the *XRN1* gene, which encodes a major 5′-to-3′ exonuclease in *Saccharomyces cerevisiae*. In *xrn1*Δ cells, *PGK1* transcripts lacking the 5′ cap structure and a few nucleotides at the 5′ end were detected after deadenylation. Second, we inserted into the *PGK1* 5′ untranslated region strong RNA secondary structures, which can slow exonucleolytic digestion and thereby trap decay intermediates. These secondary structures led to the accumulation of *PGK1* mRNA fragments, following deadenylation, trimmed from the 5′ end to the site of the secondary structure. The insertion of strong secondary structures into the 5′ untranslated region also inhibited translation of the mRNA and greatly stimulated the decay of the *PGK1* transcripts, suggesting that translation of the *PGK1* mRNA is required for its normally slow rate of decay. These results suggest that one mechanism of degradation of the *PGK1* transcript is deadenylation followed by decapping and subsequent 5′-to-3′ exonucleolytic degradation. In addition, by blocking the 5′-to-3′ degradation process, we observed *PGK1* mRNA fragments that are consistent with a 3′-to-5′ pathway of mRNA turnover that is slightly slower than the decapping/5′-to-3′ decay pathway. These observations indicate that there are multiple mechanisms by which an individual transcript can be degraded following deadenylation.

Inherent differences between the decay rates of mRNAs, as well as regulated changes in the rates of decay of individual transcripts, can significantly affect the level of gene expression in eukaryotes. To understand how these differences in mRNA decay rates are produced and regulated, it is critical to define the mechanisms of mRNA degradation. It is now clear that there are several different mechanisms of mRNA turnover in eukaryotic cells (for a review, see reference 11). One major mechanism of mRNA decay, observed for eukaryotes as diverse as mammals and yeasts, is initiated by the cytoplasmic shortening of the poly(A) tail (4, 10, 19, 23, 31, 32, 36). How deadenylation leads to degradation of the transcript body has recently been determined for the unstable yeast *MFA2* transcript. For this mRNA, deadenylation triggers a decapping reaction, which in turn exposes the entire length of the transcript to 5′-to-3′ exonucleolytic degradation (22).

The approach used to determine the mechanism of *MFA2* mRNA degradation was to monitor the decay of a pulse of newly synthesized transcripts while blocking 5′-to-3′ exonucleolytic degradation. We previously described a method using the carbon source regulation of the yeast *GAL1* upstream activating sequence (UAS) to rapidly induce, and then quickly repress, transcription of a yeast gene (10). This type of experiment, referred to as a transcriptional pulse-chase, creates a pulse of transcripts whose decay can be examined during the following chase, thus allowing the determination of precursor-product relationships. By blocking the exonucleolytic decay process, and by determining the structures of mRNA fragments that showed a precursor-product relationship with the full-length mRNA, it was possible to define the steps following deadenylation.

Two different blocks to 5′-to-3′ degradation were used in the analysis of the *MFA2* transcript. First, a poly(G) tract was inserted into the *MFA2* 5′ untranslated region (UTR). The poly(G) tract is able to stall yeast exonucleases, presumably by forming an extremely stable secondary structure (35, 41), and thereby trap decay intermediates (10, 34). Following deadenylation, fragments of the *MFA2* mRNA trimmed from the 5′ end to the site of the poly(G) insertion accumulated as full-length mRNA levels decreased. The second strategy used was to examine the decay of the *MFA2* mRNA in a yeast strain lacking a major 5′-to-3′ exonuclease encoded by the *XRN1* gene (20). In this strain, the *MFA2* mRNA is significantly more stable following deadenylation and accumulates as full-length, decapped transcripts (22). Both of these results indicate that deadenylation of the *MFA2* mRNA leads to the removal of its 5′ cap structure (decapping), exposing the transcript to 5′-to-3′ digestion by the *XRN1* exonuclease.

Since the poly(A) tail and the cap structure are found on essentially all mRNAs, this pathway could be a general mechanism for the decay of many transcripts in yeasts and potentially other eukaryotes. To determine if this deadenylation-dependent decapping pathway is common to stable and unstable mRNAs, we examined the decay of a stable yeast mRNA. We chose to analyze the *PGK1* transcript for several reasons. First, this transcript is known to require deadenylation for decay (10). Second, when a poly(G) tract is inserted into the *PGK1* 3′ UTR, a mRNA fragment corresponding to the 3′ end of the *PGK1* mRNA accumulates after deadenylation, suggesting that this mRNA is also subject to 5′-to-3′ degradation (10, 34). Finally, since the *PGK1* mRNA is one of the most stable yeast mRNAs, if this mRNA is degraded by the same pathway as the unstable *MFA2* transcript, then these studies should provide a mechanistic basis for understanding the differences in mRNA decay rates.

* Corresponding author.

To examine how the *PGK1* transcript was degraded following deadenylation, we utilized the same two strategies to trap decay intermediates used previously in the analysis of the *MFA2* mRNA. The results from the analysis of the *PGK1* mRNA indicated that there are at least two mechanisms by which this transcript can be degraded following deadenylation. One mechanism of degradation was a process in which deadenylation led to decapping of the *PGK1* mRNA followed by 5′-to-3′ exonucleolytic degradation. Thus, this mechanism appears to be a general decay pathway common to both stable and unstable transcripts, potentially regulated by both *cis*- and *trans*-acting factors. In addition, we obtained evidence which suggests the *PGK1* mRNA can also be degraded in a 3′-to-5′ direction, thus indicating that there are multiple mechanisms by which an mRNA can be degraded following deadenylation.

MATERIALS AND METHODS

Yeast strains and medium. The *Saccharomyces cerevisiae* strains used for analysis were wild-type strain yRP582 (*MAT***a** *rpb1-1 ura3-52 leu2*) and the isogenic *xrn1*Δ strain yRP689 (*MAT***a** *rpb1-1 ura3-52 leu2 XRN1*Δ*::URA3*). The yeast strains were transformed by standard techniques, and plasmids were maintained by growth in selective medium.

mRNA analysis. Steady-state mRNA experiments were performed as described previously (5). Briefly, cells were grown to mid-log phase in galactose medium, harvested, and shifted to dextrose medium at 36°C to inhibit transcription from the RNA polymerase II mutation *rpb1-1*, with an aliquot removed at each time point.

Transcriptional pulse-chase experiments used to track a synchronous pool of mRNAs were done as previously described (10, 22). Briefly, cells were grown to mid-log phase in medium containing raffinose, harvested, resuspended in medium containing galactose to induce the transcripts, and then shifted to 36°C in the presence of dextrose to shut off transcription.

mRNA was isolated as described previously (5). RNase H and polyacrylamide Northern (RNA) assays were done with 10 μg of RNA as previously described (23). Northern assay results were quantitated on a Betascope and standardized to values for scR1, an RNA polymerase III transcript (13).

Immunoprecipitations were performed on 10 μg of RNA as described previously (22, 39), using anti-m^{7}G antibodies produced by T. W. Munns (25).

Primer extensions using 20 μg of mRNA and oligonucleotide oRP95 (5′-GATCAATTCGTCGTCGTCGAATAAAGAAGACAA-3′) were done according to standard protocols with Superscript-RT (GibcoBRL).

RNase protection assays were performed as described previously (22), using plasmid pRP597, a pGEM-4Z vector containing the 5′ end of the pGPGK1 construct spanning from the *Pvu*I site 250 bases 5′ of the mRNA start site to the *Kpn*I site 550 bases into the coding region. This plasmid was linearized with *Bam*HI (at the *Pvu*I site in the clone) and transcribed with T7 RNA polymerase and [α-^{32}P]UTP to produce uniformly labeled antisense RNA. Digestions of 10 μg of total mRNA were done with RNase One (Promega) as instructed by the manufacturer.

Liquid β-galactosidase assays were done on constructs containing fusions of the *PGK1* gene to the *lacZ* coding region (see below for plasmid constructions). Cells expressing these fusion constructs were grown in medium containing galactose, harvested, and lysed, and then the resulting supernatants were assayed for β-galactosidase activity as previously described (3). Translation rates were determined by assigning the wild-type fusion a value of 100% and then calculating the relative rates of the other constructs.

Plasmids. The plasmid template used for site-directed mutagenesis of *PGK1* was created by subcloning the 5′ portion of *PGK1* from the *Bam*HI-to-*Xba*I sites of pRP170 (14) into the *Bam*HI and *Xba*I polylinker sites of the pun70 vector (12). The *Bgl*II site found within the vector sequence of pun70 was filled in with Klenow fragment to yield plasmid pRP520.

Site-directed mutagenesis, performed by standard techniques (23), was used to introduce two different *Bgl*II sites into this partial *PGK1* construct. The first, referred to as B27, was created with oligonucleotide oRP130 (5′-CATTGTTTT TAGATCTGTTGTAAAAAG-3′), placing the start of the *Bgl*II site 27 bases into the 5′ UTR to give plasmid pRP524. The second site created, B55, used oligonucleotide oRP148 (5′-TGGACAGAGATGTTTGAAG-3′) located 55 bases into the mRNA within the coding region of the transcript to give plasmid pRP599. Several insertions into the *Bgl*II sites of plasmids pRP524 and pRP599 were made and verified by sequencing. The inserted sequences are neutral tag (5′-GATCTTGTCTTCTTTATTCGACGACGACGAATT-3′), tetraloop (5′-GATCCCGCGGTTCGCCGCGG-3′), poly(G), (5′-GATCTAGGAATTTGGG GGGGGGGGGGGGGGGAATTCCT-3′), and the complementary sequence yielding poly(C). The *PGK1* portion containing the inserted sequences were then moved by subcloning the *Bam*HI-to-*Xba*I fragment into the *Bam*HI and *Xba*I sites of several vectors, all of which contain the *PGK1* gene behind the *GAL1* UAS and the *URA3* gene. The vector plasmids were pRP170, which has an inert oligonucleotide insertion in the 3′ UTR described previously (14); pRP469 (10), containing a 18-nucleotide poly(G) insertion in the 3′ UTR of *PGK1*; and pRP552, containing the same 3′ poly(G) insertion and a *LEU2* gene (24). The only insertion into the pRP170 vector was the poly(G) into the B27 site, giving plasmid pGPGK1-pRP545. Insertions into the pRP469 vector are as follows: the poly(G) into the B27 site, giving pGPGK1pG-pRP546; the stem-loop oligonucleotide into the B27 site, giving SLPGK1pG-pRP543; the B27 site with no insert, giving B27PGK1pG-pRP549; and the tagging oligonucleotide into the B55 site, giving B55T and B55TPGK1pG-pRP602. Two insertions into the *URA3*/*LEU2* vector pRP552 were B27poly(G)–pGPGK1pG-pRP619 and B55 Tag–B55TPGK1pG-pRP603.

The plasmid used to create a riboprobe specific for the 5′ end of the transcript was pRP620, which contains the 5′ end of the B55TPGK1N103 transcript (24) from the *Pvu*I site 5′ of the gene to the *Kpn*I site within the coding region inserted into the pGEM-4Z vector (Promega). Digestion with *Eco*RI and transcription with T7 RNA polymerase and [α-^{32}P]UTP produced uniformly labeled complementary RNA.

PGK1-lacZ fusion constructs were made by fusing in frame the modified 5′ *PGK1* portions described above from the *Bam*HI site to the 5′-most *Sal*I site, 725 bases into the *PGK1* coding region, into the vector pRP186 (3). This vector contains the *lacZ* coding region from pRP186 with an *Xho*I linker introduced at the 5′ end and an *Xba*I site introduced at the 3′ end. The transcription terminator of the *PGK1* gene is connected to the *lacZ Xba*I site by an *Xba*I linker inserted at the *Bgl*II site in the *PGK1* 3′ UTR. The fusion proteins and plasmids constructed are as follows: PGK1-Z, pRP556; B27PGK1-Z, pRP557; B27CPGK1-Z, pRP560; B27pGPGK1-Z, pRP559; B27TPGK1-Z, pRP613; and B27SLPGK1-Z, pRP558.

RESULTS

Analysis of the decay of the *PGK1* mRNA in an *xrn1*Δ strain. In the first experiment performed to determine the step following poly(A) tail shortening of the *PGK1* mRNA, we examined the decay of transcripts in strains lacking the major yeast 5′-to-3′ exonuclease *XRN1*. If the *XRN1* gene product, Xrn1p, also functions in the degradation of the *PGK1* mRNA, then an *xrn1*Δ strain should accumulate the products of the nucleolytic cleavage which follows deadenylation.

To determine if the deletion of the *XRN1* gene had any effect on the overall half-life of the transcript, we measured the decay rate of the *PGK1* transcript in an *xrn1*Δ strain. To detect decay products that arise by 5′-to-3′ degradation, we examined the decay of a *PGK1* transcript containing a poly(G) tract in its 3′ UTR (termed PGK1pG) which was previously shown not to affect the half-life of the mRNA (10). The wild-type and isogenic *xrn1*Δ strains expressing the PGK1pG transcript under control of the *GAL1* UAS were grown in media containing galactose as a carbon source to mid-log phase at 24°C (steady-state conditions). Since these strains also carry a temperature-sensitive RNA polymerase II allele (*rpb1-1*), transcription was repressed by the addition of glucose and simultaneously shifting to 36°C (5). As has been reported previously for the endogenous *PGK1* mRNA (20), the *xrn1*Δ mutation has essentially no effect on the decay rate in the full-length PGK1pG mRNA (Fig. 1) compared with the rate in an isogenic wild-type strain. However, the amount of the decay intermediate corresponding to the 3′ portion of the *PGK1* mRNA stabilized by the poly(G) tract in the 3′ UTR was reduced from approximately 30% of the total mRNA at 0 min in the wild-type cells to <5% in the *xrn1*Δ cells (Fig. 1, lower band in each panel). This result suggests that the *XRN1* nuclease normally produces this decay intermediate. However, digestion by Xrn1p must not be a rate-limiting step in *PGK1* mRNA decay since the *xrn1*Δ mutation did not affect the half-life of the full-length mRNA (see below and Discussion). It should be noted that since we can detect some of the 3′ poly(G) decay fragment in the *xrn1*Δ strain on long exposures (data not shown; see also Fig. 7), there is another 5′-to-3′ exonuclease that can substitute, albeit inefficiently, for Xrn1p (24).

To observe the mechanism of decay of the PGK1pG mRNA in *xrn1*Δ cells more thoroughly, we performed a transcriptional

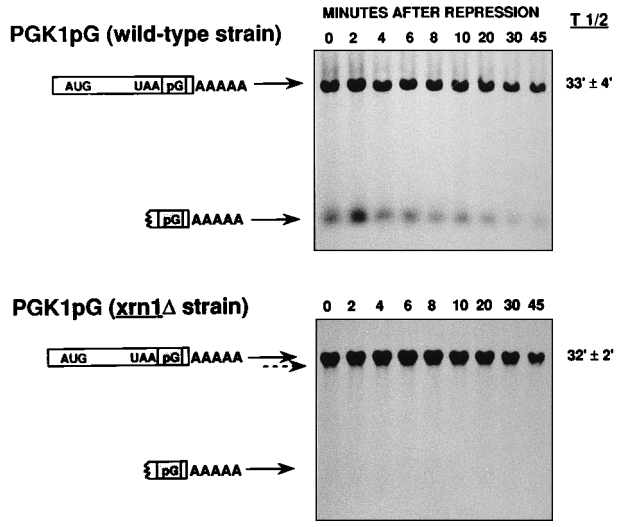

FIG. 1. Deletion of the 5′-to-3′ exonuclease *XRN1* reduces the levels of the 3′ poly(G) decay intermediate. Steady-state half-life measurements of the PGK1pG mRNA in the wild-type and *xrn1*Δ strains were determined from agarose Northern gels. On the left are cartoons of the mRNA species present in each band, with the shaded box representing the poly(G) (pG) insertion in the 3′ UTR. The top band represents the full-length mRNA, and the lower band is a decay intermediate which accumulates as a result of the 3′ poly(G) insertion. The dashed arrow shows the position of an additional decay intermediate produced from an alternative 3′-to-5′ decay pathway (see Fig. 8 and 9). The numbers above the lanes indicate minutes after transcriptional repression. The average value (minutes) of the half-life for the full-length transcript from at least four experiments in each strain is given on the right. Northern gels were probed with oligonucleotide oRP121 (5′-AATTCCCCCCCCCCCCCCCCCCA-3′), which is complementary to the 3′ UTR poly(G) insertion.

pulse-chase by using the *GAL1* UAS to transcribe the PGK1pG mRNA for a brief period of time (10). If deadenylation triggers decapping of the *PGK1* transcript, then we would expect to detect transcripts lacking the cap structure in the *xrn1*Δ strain. Alternatively, if deadenylation leads to endonucleolytic cleavage as has been suggested previously (34), then the initial products of that endonucleolytic cleavage event should accumulate. To allow the 5′ end of the PGK1pG transcript to be distinguished from endogenous *PGK1* transcripts, we inserted an oligonucleotide near its 5′ end (referred to as B55T; see Materials and Methods). This insertion has no effect on mRNA decay (reference 24 and data not shown).

Examination of the B55TPGK1pG transcripts from a transcriptional pulse-chase in an *xrn1*Δ strain (Fig. 2A) indicated that these *PGK1* transcripts remain full length, within the resolution of an agarose Northern gel. This observation suggests that any cleavage events that occurred after deadenylation made only minor changes (<100 bases) to the overall size of the *PGK1* mRNA and therefore are likely to be near the transcript's termini.

To examine the 3′ end and the poly(A) tail of the PGK1pG transcripts, we cleaved the mRNA near the 3′ end with an oligonucleotide and RNase H and analyzed these cleavage products on an acrylamide northern gel. The deadenylation rates are similar in the wild-type and *xrn1*Δ strains (Fig. 2B). As in the analysis of the mRNA at steady state (Fig. 1), the amount of mRNA fragment stabilized by the poly(G) insertion in the 3′ UTR is substantially reduced in the *xrn1*Δ cells and can be observed only on overexposed autoradiograms (data not shown).

We determined if the *PGK1* mRNA is decapped following deadenylation by examining the 5′ ends of the B55TPGK1pG mRNA in the *xrn1*Δ strain. To resolve size differences at the 5′ ends of the transcripts, we cleaved the mRNA with RNase H and an oligonucleotide near the 5′ end and analyzed the cleavage products on an acrylamide Northern gel. In this experiment, we used a probe that hybridizes to the endogenous *PGK1* mRNA (lower band in Fig. 2C) as well as the B55TPGK1pG mRNA (upper band in Fig. 2C). The important observation is that only in the *xrn1*Δ cells is a new B55TPGK1pG mRNA species that is slightly shorter at the 5′ end observed (upper dashed arrow in Fig. 2C). Transcripts with the shortened 5′ end are first easily detectable at 20 min during the chase and are more predominant at later time points when the level of transcripts with the full-length 5′ end has declined significantly. The small amount of these trimmed transcripts observed in the early time points is due to a low level of transcription during growth prior to the transcriptional pulse as well as to the degradation of transcripts produced earlier in the pulse than the bulk of the mRNA. Thus, these 5′-trimmed transcripts begin to accumulate substantially only after deadenylation (compare Fig. 2B and C). Shortened species are also seen with the endogenous *PGK1* transcript (lower dashed arrow in Fig. 2C), indicating that this 5′-end trimming is not specific to the B55TPGK1pG transcript. The 5′-trimmed species are present throughout the time course for the endogenous *PGK1* mRNA because this transcript is not under *GAL* control and therefore is expressed continuously prior to transcriptional repression by *rpb1-1*. The minor band located between the major band and this 5′-trimmed species which is present throughout the time course in both wild-type and *xrn1*Δ cells is probably due to heterogeneity in the cleavage by RNase H since it is not observed by primer extension analysis (see below). Taken together, the results presented in Fig. 2 suggest that deadenylation of *PGK1* mRNA leads to a cleavage event very near the 5′ end which removes the cap structure and exposes the transcript to 5′-to-3′ exonucleolytic degradation.

To verify that these *PGK1* transcripts shortened at the 5′ end were indeed lacking the cap structure, we assayed for the presence of the cap at early and late times in the transcriptional pulse-chase, using antibodies specific for the 5′ cap structure. The B55TPGK1pG mRNA isolated at the 0-min time point from the wild-type and *xrn1*Δ strains was immunoprecipitated, demonstrating that the newly synthesized transcripts are capped in both strains (Fig. 3, lanes 2 and 5). At 80 min, after the mRNA has been deadenylated and has begun to decay, transcripts which are trimmed at the 5′ end are now detected in the supernatant lanes in the *xrn1*Δ strain (Fig. 3, lanes 9 and 12), indicating that these mRNAs are indeed uncapped.

Primer extension analysis of the B55TPGK1pG mRNA indicates that the predominant trimmed species is shorter than the primary transcript at the 5′ end by two nucleotides (Fig. 4). Transcripts trimmed by two nucleotides are also seen for the endogenous *PGK1* mRNA by Northern analysis (Fig. 2C). These observations suggest that at least some of the *PGK1* mRNA is decapped following deadenylation (see Discussion).

Analysis of the decay of *PGK1* transcripts containing secondary structures in the 5′ UTR. The second, and complementary, approach that we used to determine the decay events that follow deadenylation was to insert a poly(G) tract into the 5′ UTR of the *PGK1* mRNA. As described above, the poly(G) tract is capable of forming a structural barrier to yeast exonucleases (10, 23, 31a, 34). If deadenylation led to decapping of the *PGK1* transcripts followed by 5′-to-3′ digestion, then we would expect transcripts containing a 5′ UTR poly(G) insertion to accumulate as mRNA fragments degraded at the 5′ end into the poly(G) structure following deadenylation.

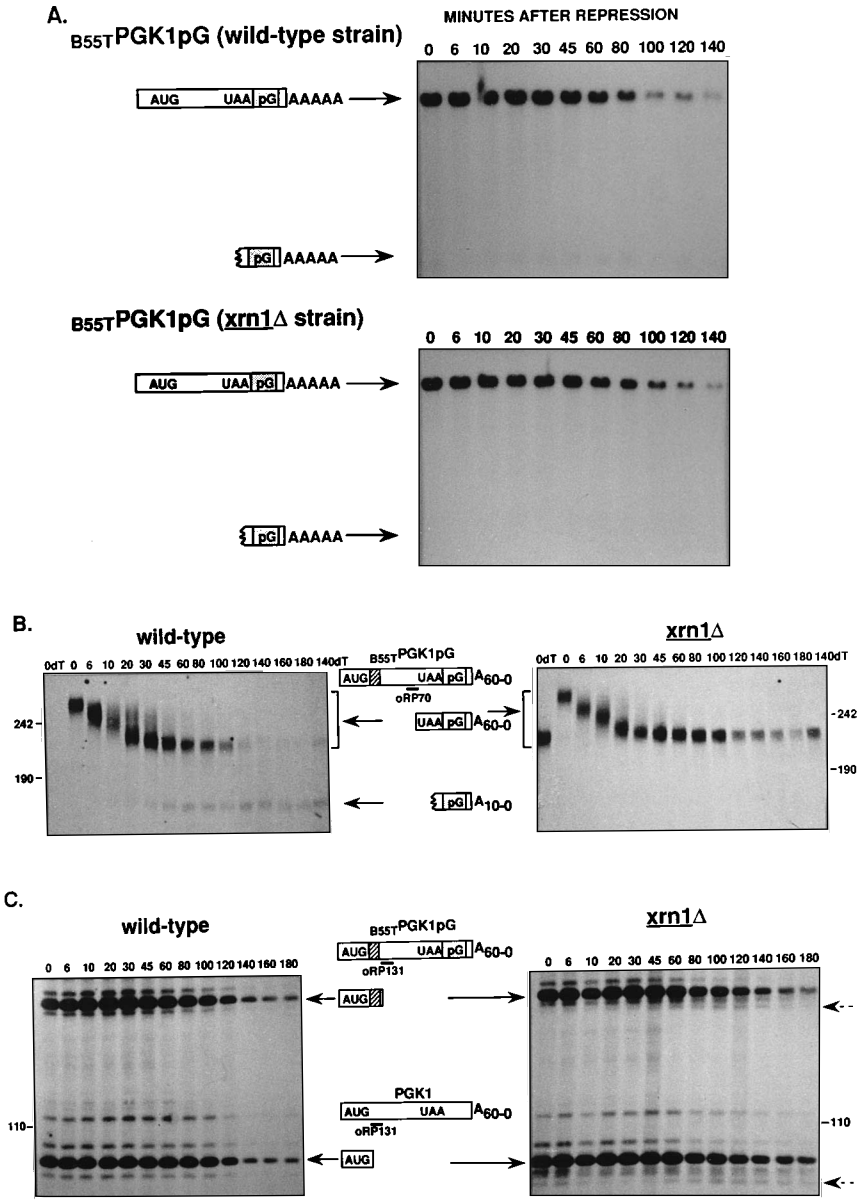

FIG. 2. Transcriptional pulse-chase analysis of the PGK1pG mRNA in the *xrn1*Δ strain. (A) The B55TPGK1pG mRNA, which contains an inert 5′-end insertion, from transcriptional pulse-chase experiments in the wild-type and *xrn1*Δ strains examined on agarose Northern gels. Time points taken after a 10-min transcriptional induction and subsequent repression are shown above the lanes. Cartoons on the left represent the full-length and 3′ poly(G) (pG)-stabilized mRNA species. In the bottom panel, the 3′ poly(G) decay intermediate is visible only on very long exposures, but the location is designated for comparison. The Northern gels were probed with oligonucleotide oRP121 (see Fig. 1). (B) Deadenylation rate of the 3′ end of the B55TPGK1pG transcript from transcriptional pulse-chase experiments in the wild-type or *xrn1*Δ strain. The cartoons between the panels depict the full-length mRNA at the top; below are the two fragments observed in the polyacrylamide Northern gels. The top fragment was produced by cleavage of the full-length mRNA with RNase H and oligonucleotide oRP70 (5′-CGGATAAGAAAGCAACAC CTGG-3′). This cleavage shortens the mRNA enough to visualize small size differences at the 3′ end. The bottom fragment is the decay intermediate stabilized by the poly(G) insertion in the 3′ UTR. The numbers after the A's in the cartoons represent the range of poly(A) tail sizes found on each mRNA species determined by comparison with the oligo(dT) lanes, in which the poly(A) tails have been completely removed with cleavage by RNase H, oligonucleotide oRP70, and oligo(dT). In the left panel there is no 0dT lane loaded on the gel. Minutes after transcriptional repression are given above the lanes, and DNA size markers (in nucleotides) are shown. The blots were probed with oRP121 (Fig. 1). (C) The 5′ ends of the B55TPGK1pG and endogenous *PGK1* transcripts from the same transcriptional pulse-chase experiments as in panel B are shown. After cleavage with RNase H and oligonucleotide oRP131 (5′-GAAGTCAACTTAGATGAAGAC-3′), which is about 100 bases from the 5′ end of the *PGK1* mRNA, the mRNAs were analyzed on polyacrylamide Northern gels. The Northern gels are probed with a riboprobe complementary to the 5′ third of the *PGK1* transcript to visualize both endogenous *PGK1* and the B55TPGK1pG transcripts. The top cartoon between the panels shows the full-length B55TPGK1pG construct, the position of oligonucleotide oRP131, as well as the 5′ tagging insertion (striped box) and 3′ UTR poly(G) insertion (shaded box). The mRNA species resulting from cleavage of the B55TPGK1pG mRNA with oligonucleotide oRP131 and RNase H is depicted immediately below. The endogenous *PGK1* transcript is also diagrammed, with its cleaved 5′ portion shown below. The A's after the mRNA cartoons represent the population of poly(A) tails found on the mRNAs. The dashed arrows at the right of the *xrn1*Δ panel show the positions of the mRNA species shortened at their 5′ ends. Primer extension analysis suggests that the minor bands located above the major band for both the endogenous and B55TPGK1pG transcripts in wild-type and *xrn1*Δ strains represent additional transcriptional start sites, whereas the minor band between the major band and the 5′-trimmed species is due to imprecise cleavage by RNase H. DNA size markers (in nucleotides) are shown beside the panels. Time points are given above the lanes in minutes after transcriptional repression.

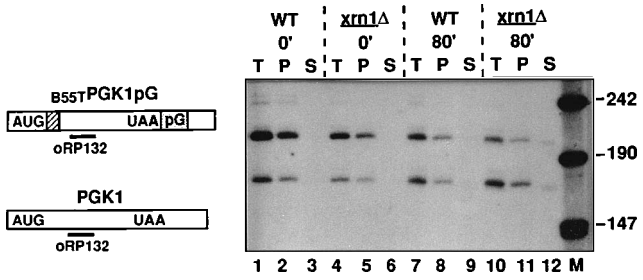

FIG. 3. The *PGK1* mRNAs shortened at the 5′ end which accumulate in the *xrn1*Δ strain are decapped. The acrylamide Northern gel shows the 5′ ends of both endogenous *PGK1* and the B55TPGK1pG mRNAs from transcriptional pulse-chase experiments after immunoprecipitation with anticap antibodies. The mRNAs were cleaved with RNase H and oligonucleotide oRP132 (5′-GGTTG GCAAAGCAGC-3′) to easily distinguish size differences at the 5′ end. The cartoons at the left show the full-length mRNA represented in each band. The top bands correspond to the B55TPGK1pG transcript; the lower bands are the endogenous *PGK1* mRNAs. pG, poly(G) site. The strains, either wild-type (WT) or *xrn1*Δ, and the time points in minutes after transcriptional repression are listed above the lanes. Total (T), pellet (P), and supernatant (S) fractions after immunoprecipitation are designated above the lanes. DNA size markers (in nucleotides) are shown in lane M. The other lanes are labeled numerically for reference purposes. The Northern gel was probed with a riboprobe specific to the 5′ third of *PGK1* mRNA (see Fig. 2C).

To insert specific sequences into the *PGK1* 5′ UTR, we created a *Bgl*II site at nucleotide 27 of the mRNA by site-directed mutagenesis (see Materials and Methods). The point mutation created in this construct had no effect on the turnover of the *PGK1* mRNA (data not shown). Subsequently, we inserted into the B27 *Bgl*II site sequences containing an 18-nucleotide poly(G) tract (referred to as pGPGK1). In addition, we also inserted sequences capable of forming a stem-loop that is sufficient to block translation but only minimally blocks exonucleolytic digestion (referred to as SLPGK1) (3).

Since the insertion of strong stem-loops and poly(G) tracts in the 5′ UTRs of yeast mRNAs has been previously shown to inhibit translation initiation (3, 7, 33, 34), we first examined the effects of these insertions on translation of the *PGK1* transcripts. We replaced a portion of the *PGK1* coding region in

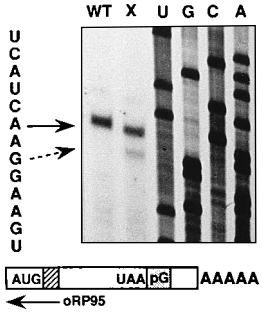

FIG. 4. B55TPGK1pG transcripts in the *xrn1*Δ strain are shortened at the 5′ end. Shown is primer extension analysis of B55TPGK1pG mRNAs isolated from steady-state cultures of the wild-type (WT) and *xrn1*Δ (X) strain at 45 min after transcriptional repression, when the shortened fragments are most abundant. Extensions were done with oligonucleotide oRP95 (see Materials and Methods), which is complementary to the B55T tagging insertion near the 5′ end of the mRNA. The sequence of the B55TPGK1pG DNA with oRP95 is in lanes U, G, C, and A, labeled as the sense strand of the mRNA. A portion of the corresponding sequence is listed at the right from 5′ (top) to 3′ (bottom). The major 5′ end seen in both strains is identified by the solid arrow, and the additional species present in the *xrn1*Δ strain is marked with the dashed arrow. The cartoon below depicts the relative location of the primer to the full-length mRNA, with the B55T sequence shown as a striped box and the poly(G) (pG) sequence shown as a shaded box.

TABLE 1. Results of quantitative β-galactosidase assays of *PGK1-lacZ* fusion constructs[a]

5′ insertion construct	% *lacZ* fusion translation (mean ± SD)	$t_{1/2}$ (min)[b]
PGK1	100	35
B27PGK1	119 ± 14.9	33
B27SLPGK1	0.014 ± 0.011	3.5
B27pGPGK1	0.0035 ± 0.0023	7
B27pCPGK1	146 ± 2.5	28
B27TPGK1	ND	30

[a] Abbreviations: ND, not determined; B27, *Bgl*II site; pC, poly(C) insertion; T, neutral tagging sequence insertion; SL, stem-loop insertion; pG, poly(G) insertion.

[b] Half-life values of the corresponding *PGK1* transcript not fused to *lacZ*. (The *PGK1* transcripts, except pCPGK1, contained a 3′ poly(G) insertion.) To distinguish the half-life of the full-length B27pGPGK1 mRNA from that of the stable decay fragment which is shortened from the 5′ end to the 5′ poly(G) insertion, the decay rate of the full-length 5′ end was determined by polyacrylamide Northern analysis after cleavage with RNase H and oRP131 (see Fig. 5B).

each construct with the *lacZ* reporter gene and measured the levels of β-galactosidase protein by enzymatic assay. By comparison with the wild-type fusion (assigned a relative translation rate of 100%), both the stem-loop and the poly(G) insertions prevented nearly all mRNA translation, reducing the relative translation rates to 0.014 and 0.0035%, respectively (Table 1). This effect was specific to the sequences capable of forming strong RNA structures since insertion of a poly(C) sequence at the same position in the 5′ UTR did not reduce β-galactosidase activity. These results are consistent with prior observations (3, 7, 33, 34) and indicated that both the stem-loop and poly(G) insertions in the *PGK1* 5′ UTR severely inhibit translation, presumably by blocking scanning of the 40S subunit (18).

Secondary structure insertions in the 5′ UTR destabilize the *PGK1* mRNA. Since translation is known to be required for the normal degradation of many, but not all, mRNAs (3, 8, 27, 29), we determined the effect of translation inhibition on the decay of the *PGK1* mRNA. In contrast to other mRNAs whose decay is slowed by the inhibition of translation in *cis* (1, 30, 37, 38), both the SLPGK1 ($t_{1/2}$ = 3.5 min) and pGPGK1 ($t_{1/2}$ = 7 min) transcripts were degraded significantly faster than the parental *PGK1* mRNA ($t_{1/2}$ = 35 min) (Table 1). These changes in decay rate were not observed with the insertion of either the poly(C) tract or the neutral tagging oligonucleotide, which are incapable of forming a strong RNA secondary structure (Table 1 and data not shown). These results suggest that the stability of the *PGK1* transcript requires translation of the mRNA (see Discussion).

Secondary structure insertions in the 5′ UTR accelerate deadenylation and decapping. To examine the mechanism by which the SLPGK1 and pGPGK1 mRNAs were degraded, we examined their turnover in a transcriptional pulse-chase. In particular, we wanted to determine if mRNA fragments which were trimmed from the 5′ end to the poly(G) secondary structure arose after deadenylation. In addition, we wanted to determine the mechanistic basis for the accelerated decay pathway of the SLPGK1 and pGPGK1 mRNAs. In each case, the *PGK1* transcript analyzed also contained a poly(G) tract in its 3′ UTR to allow detection of any decay products arising by 5′-to-3′ exonucleolytic degradation.

Analysis of transcriptional pulse-chase experiments for the SLPGK1pG and pGPGK1pG transcripts revealed several important observations. First, by examining the 3′ end of the

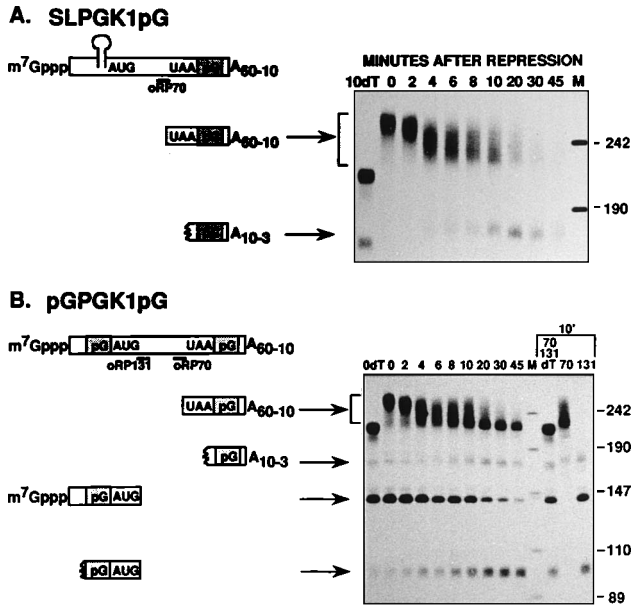

FIG. 5. Secondary structures inserted in the 5′ UTR of the *PGK1* mRNA accelerate deadenylation and decay. (A) Deadenylation of the SLPGK1pG mRNA from a transcriptional pulse-chase in the wild-type strain. The mRNA was cleaved with oligonucleotide oRP70 (Fig. 2) and RNase H and then analyzed on a polyacrylamide Northern gel to visualize the 3′ ends of the transcripts with the oligonucleotide probe oRP121 (Fig. 1). The top cartoon depicts the full-length SLPGK1pG mRNA, with the 5′ UTR stem-loop structure, the 3′ UTR poly(G) (pG) insertion, and the position of the oRP70 oligonucleotide marked. The smaller cartoons show the mRNA species visible in each band on the Northern gel, with the poly(A) tail lengths of each given as determined by comparison with RNA from the 10-min time point cleaved with oligo(dT) (10dT) from which the poly(A) tail has been removed. Time points are listed above the lanes in minutes after transcriptional repression. The sizes (in nucleotides) of the DNA markers run in lane M are at the right. (B) Deadenylation analysis on pGPGK1pG mRNAs from a transcriptional pulse-chase experiment. This mRNA was cleaved with RNase H and two oligonucleotides, oRP131 at the 5′ end and oRP70 at the 3′ end. The cartoons on the left show the full-length mRNA and the species present in each band on the Northern gel. Time points after transcriptional repression are shown above the lanes. The first lane on the gel is RNA from the 0-min time point cleaved with oligo(dT), in addition to oligonucleotides oRP70 and oRP131, to remove the poly(A) tail. Lane M shows the DNA size markers listed on the right in nucleotides. The three lanes on the right are mRNA from the 10-min time point cleaved by RNase H with oligonucleotides oRP70 and oRP131 and oligo(dT) together or with either oRP70 or oRP131 alone to demonstrate the specificity of each mRNA species. The Northern gel was probed with oligonucleotide oRP121 (Fig. 1), which is complementary to the poly(G) sequence.

transcript on an acrylamide Northern gel, we observed that in both cases the deadenylation rate is increased three- to four-fold compared with the wild-type mRNA rate (compare Fig. 5 with Fig. 2B). On the basis of the sizes of the shortest poly(A) tails present at each time point, the rate of poly(A) shortening of the SLPGK1pG and pGPGK1pG mRNAs is approximately 15 adenylate residues per minute. In comparison, the parental *PGK1* transcript deadenylates at a rate of approximately four adenylate residues per minute (10). In addition, the population of transcripts containing strong secondary structures in the 5′ UTR deadenylated in a more heterogeneous manner than normally observed for the *PGK1* transcript. Together with the results from the *lacZ* fusion mRNAs these observations suggest that translation in *cis* is required for the slow deadenylation rate normally observed for the *PGK1* mRNA (see Discussion).

A second important point is that these transcripts did not begin to decay until after deadenylation. This conclusion is based on the observation that the level of the transcripts did not begin to decrease until after some of the mRNA had been deadenylated (Fig. 5). In addition, for both the SLPGK1 and pGPGK1 mRNAs, decay products arising from 5′-to-3′ degradation began to accumulate after deadenylation. This result is most easily seen for the SLPGK1pG transcript: the decay product stabilized by the poly(G) tract in the 3′ UTR appeared only after the mRNA was deadenylated (Fig. 5A). Moreover, at the time when this mRNA fragment first appears, it has an oligo(A) tail, even though the total mRNA population at this time point consists of transcripts with both long and short poly(A) tails (Fig. 5A). In contrast, in the deadenylation-independent decay pathway promoted by the presence of early nonsense codons (24), similar decay intermediates stabilized by the poly(G) tract in the 3′ UTR are produced, but these intermediates have long poly(A) tails. For the pGPGK1pG construct, a decay product arising by 5′-to-3′ decay (described below) also accumulated following deadenylation (Fig. 5B, lowest band). Low levels of this species were observed at the 0- and 2-min time points before the majority of the population was deadenylated, presumably because the transcriptional pulse-chase was not completely synchronous (note that a fraction of the mRNA at time zero has already been deadenylated). However, since the 3′ ends of this species cannot be distinguished from the remaining full-length mRNA, we are unable to determine the length of its poly(A) tail. We conclude, as has been observed for the *PGK1* mRNA without insertions in its 5′ UTR (10), that only oligoadenylated transcripts are substrates for the next step in the decay pathway. Therefore, although the degradation of the *PGK1* mRNA has been accelerated, presumably as a result of the inhibition of translation, its decay still requires deadenylation.

We also noted that the decay of the oligoadenylated species of the transcripts with secondary structures in their 5′ UTRs is significantly faster than that of the parental *PGK1* transcript. Unlike the wild-type transcript, the SLPGK1pG mRNA does not persist as an oligo(A) species (compare Fig. 2B and 5A). In the case of the pGPGK1pG mRNA, the stability of the oligoadenylated transcript is obscured because the oligo(A) fragment is derived from RNase cleavage of the 3′ end of both the full-length mRNA and the mRNA fragments shortened at the 5′ end in to the poly(G) tract in the 5′ UTR (see below). However, examination of the full-length 5′ end of the pGPGK1pG mRNA (by cleavage with an oligonucleotide and RNase H near the 5′ end) suggests that this transcript is also relatively unstable once it is deadenylated (Fig. 5B, third band). The rapid degradation of the deadenylated forms of the SLPGK1pG and pGPGK1pG mRNAs suggests that the slow decay of the *PGK1* mRNA after deadenylation also requires translation in *cis* (see Discussion).

To determine if the pGPGK1pG mRNA is decapped following deadenylation, we examined the 5′ end of the transcript on an acrylamide Northern gel after cleavage of the mRNA near the 5′ end with an oligonucleotide and RNase H. As shown in Fig. 5B, at early times in the transcriptional pulse-chase, the transcript is full-length at the 5′ end (Fig. 5B, third band) and has a long poly(A) tail (upper band). After deadenylation (8 to 10 min), a new band of the appropriate size to be shortened from the 5′ end in to the start of the poly(G) insertion begins to accumulate (Fig. 5B, bottom band). This fragment is dependent upon cleavage with the 5′ oligonucleotide and RNase H (Fig. 5B, lanes labeled 131 and 70), indicating that it is specific to the 5′ end of the mRNA. The level of this new 5′-shortened species increased as the level of the full-length 5′ end decreased, suggesting that it is derived from the full-length 5′ end and is therefore a product of mRNA decay.

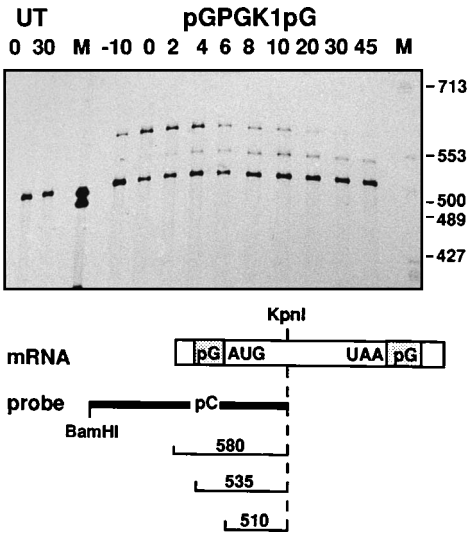

FIG. 6. RNase protection of the 5′ end of the pGPGK1pG mRNA shows 5′-to-3′ decay of the message. The pGPGK1pG mRNA from a transcriptional pulse-chase performed in the wild-type strain was protected with an RNA probe specific for the 5′ end of the transcripts. Depicted below the panel is a cartoon of the full-length mRNA showing the relative positions of the poly(G) (pG) insertions and pertinent restriction sites. The riboprobe which contained the complementary poly(C) (pC) sequence is shown as a thick line. The approximate size of each protected fragment is indicated below. UT refers to the untransformed parental strain, which expresses only the endogenous *PGK1* transcript, which protects a 510-nucleotide band (the smallest protected band in each lane) because it does not contain the poly(G) insertion. The remaining lanes are from a transcriptional pulse-chase of pGPGK1pG mRNA. Time points refer to minutes after transcriptional repression. Some of the DNA size markers run in the lanes M are listed at the right in nucleotides.

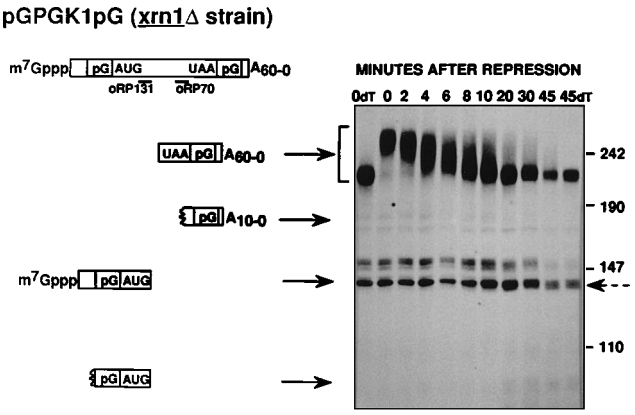

FIG. 7. The pGPGK1pG mRNA in the *xrn1*Δ strain accumulates as a deadenylated, oligo(A) species shortened at the 5′ end. The polyacrylamide Northern gel shows the deadenylation and shortening at the 5′ end of the pGPGK1pG mRNA from a transcriptional pulse-chase in the *xrn1*Δ strain. Cartoons at the left show the full-length mRNA with the poly(G) (pG) structures (shaded boxes) and positions of the two oligonucleotides, oRP70 and oRP131 (Fig. 2), used to cleave the mRNA with RNase H. The mRNA species present in each band of the gel is shown at the left, with the corresponding poly(A) tail sizes. The minor bands above the band representing the full-length 5′ end results from pGPGK1pG mRNA having multiple transcriptional start sites. DNA size markers are indicated at the right in nucleotides, and the time points are given in minutes after transcriptional repression. The first and last lanes are also cleaved with oligo(dT) to remove the poly(A) tails. The dashed arrow on the right marks the position of the shortened 5′ ends of the transcripts. The Northern gel was probed for the poly(G) insertions with oligonucleotide oRP121 (Fig. 1).

RNase protection assays on the 5′ end of the pGPGK1pG mRNA demonstrated that this decay product corresponds to an mRNA fragment trimmed to the 5′ side of the poly(G) tract in the 5′ UTR (Fig. 6).

On the basis of all of these results, we conclude that the pGPGK1pG mRNA is cleaved near the 5′ end following deadenylation and prior to 5′-to-3′ exonucleolytic digestion. It should be noted that since the pGPGK1pG mRNA is more unstable than the *PGK1* mRNA, we cannot rule out the formal possibility that these 5′ UTR insertions have changed the mechanism by which the *PGK1* transcript is degraded. However, since decapped transcripts accumulated in the *xrn1*Δ strain following deadenylation, the simplest interpretation is that the insertions have changed the rate of mRNA decay but not the mechanism. These results together argue that the *PGK1* mRNA can be decapped following deadenylation.

A prediction based on the results presented above is that in an *xrn1*Δ strain, the pGPGK1pG mRNA should give rise to mRNA fragments cleaved at the 5′ end following deadenylation, but that these fragments would not be further degraded in to the poly(G) tract in the 5′ UTR. To test this hypothesis, we performed a transcriptional pulse-chase on the pGPGK1pG mRNA in the *xrn1*Δ strain. As can be seen in Fig. 7, following deadenylation, transcripts shortened slightly at the 5′ end accumulated, whereas only minute amounts of the mRNA fragments shortened to the poly(G) tract in the 5′ UTR were produced (compare Fig. 5B and 7). Consistent with a role for deadenylation in triggering the 5′ decapping reaction, the shortened 5′ ends are now observed at an earlier time than in the wild-type transcript (Fig. 2C), corresponding to the increased deadenylation rate of the pGPGK1pG mRNA. These experiments provide additional evidence that deadenylation can trigger decapping of the *PGK1* transcripts, thus allowing degradation of the body of the mRNA by Xrn1p.

The *PGK1* transcript can be degraded from the 3′ end. The results discussed above all suggest that one mechanism of decay for the *PGK1* transcript is a deadenylation-dependent decapping reaction followed by 5′-to-3′ exonucleolytic decay. We have previously presented evidence that *PGK1* transcripts that contain early nonsense codons ($PGK1_{N103}pG$) can also be degraded from the 3′ end (24) when the major 5′-to-3′ decay pathway is blocked. The key observation was that in *xrn1*Δ cells, $PGK1_{N103}pG$ transcripts shortened from the 3′ end could be observed, with the predominant species possessing a 3′ end at the 3′ side of the poly(G) tract in the 3′ UTR. We explored the possibility that *PGK1* transcripts without nonsense codons could also be degraded through this mechanism by examining the transcripts present when 5′-to-3′ exonucleolytic degradation was blocked. We limited 5′-to-3′ exonucleolytic digestion by three independent methods: (i) removing the *XRN1* nuclease by deletion of its gene, (ii) blocking exonucleases physically by insertion of a poly(G) tract in the 5′ UTR, or (iii) adding cycloheximide at the time of transcriptional inhibition, which can inhibit the decapping reaction in yeast cells (3). As shown in Fig. 8, when any of these three methods was used and the decay of the *PGK1* mRNA with a poly(G) tract in its 3′ UTR was analyzed under steady-state conditions, a new mRNA fragment of approximately 1.3 kb was observed. Consistent with this fragment arising through 3′-to-5′ degradation, the presence of this 1.3-kb decay intermediate was dependent upon the poly(G) structure in the 3′ UTR, which presumably blocks further exonucleolytic decay.

This 1.3-kb mRNA species was the same size as the mRNA fragment that we previously detected when 5′-to-3′ degradation was blocked on mRNAs containing early nonsense codons (24). In that analysis, we were able to map the 3′ ends of the mRNA fragment by cleaving the mRNA near the 3′ end with

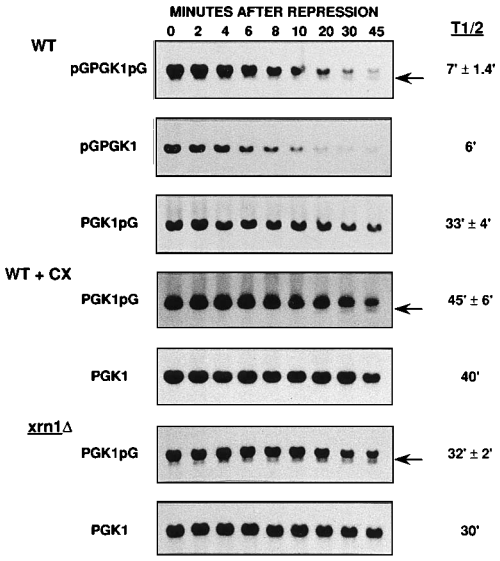

FIG. 8. An additional decay intermediate is detected when the 5′-to-3′ exonucleolytic degradation pathway is inhibited. Examination of the mRNAs present under steady-state conditions for several *PGK1* mRNAs with and without 5′ and/or 3′ poly(G) insertions are shown. The strains in which the experiments were performed are designated on the left as wild-type (WT), wild-type plus cycloheximide addition to 10 μg/ml at the time of transcriptional repression (WT + CX), and *xrn1*Δ. Time points are in minutes after transcriptional repression. Half-life measurements (minutes) and standard errors are listed to the right of each panel. Half-lives of the constructs showing additional decay intermediates were determined by measuring only the full-length transcripts. The arrows on the right designate the additional decay product observed. The Northern gels were probed with oligonucleotide oRP121 in all cases except that the WT + CX *PGK1* transcript was probed with oligonucleotide oRP42 (5′-CGATCCGCTTA ATACTGACGCTCTCGCACCAT-3′), which is homologous to a neutral tag sequence previously inserted into the 3′ UTR (14), and the endogenous *xrn1*Δ *PGK1* transcript was probed with oligonucleotide oRP132 (Fig. 3), homologous to the 5′ end of the *PGK1* mRNA.

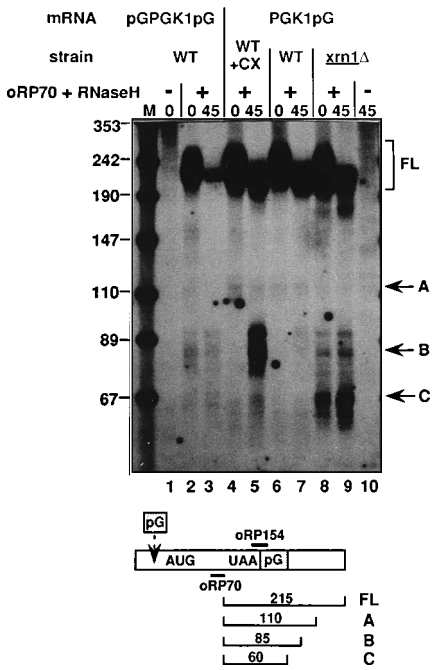

FIG. 9. The *PGK1* mRNA can be degraded by a 3′-to-5′ decay pathway. The 3′ ends of steady-state mRNAs were mapped by cleavage with RNase H and oligonucleotide oRP70 in wild-type (WT) and *xrn1*Δ strains. Lanes are numerically labeled at the bottom for reference. The mRNAs run in each lane from the designated time points are listed above the lanes. In lanes 4 and 5, cycloheximide (CX) was added to wild-type cells to 10 μg/ml at 0 min. The mRNAs were cleaved with oligonucleotide oRP70 and RNase H (except for lanes 1 and 10, in which cases no oligonucleotide was added). This Northern gel was probed with oligonucleotide oRP154 (5′-CCCCCCAAATTCCTTCGATTTC-3′), which is specific for the 5′ portion of the 3′ UTR poly(G) insertion. DNA size markers (in nucleotides) are shown in lane M. The full-length (FL) mRNA and decay intermediate bands A, B, and C are shown with arrows and correspond to the approximate-size fragments shown in the cartoon below. This cartoon shows the full-length mRNA containing the poly(G) (pG) insertions [the 5′ poly(G) indicated by an arrow] and the locations of oligonucleotides oRP70 and oRP154. The approximate sizes of the three decay intermediates A, B, and C are given.

an oligonucleotide and RNase H, thus allowing resolution of small size differences at the 3′ end on acrylamide Northern gels. We used the same approach to map the 3′ end of the 1.3-kb fragment observed in RNA obtained from steady-state cultures at 0 and 45 min after transcriptional inhibition. As shown in Fig. 9 (lanes 8 and 9), for the PGK1pG transcript in an *xrn1*Δ strain, two major sets of new 3′ ends are observed. One set of ends, previously referred to as band B (24), corresponds to a clustered set of 3′ ends within the 3′ UTR. The second major set of ends maps to the 3′ side of the poly(G) tract in the 3′ UTR (band C). These same species are observed with the pGPGK1pG transcript in wild-type cells (lanes 2 and 3). The levels of these fragments are lower in the case of the pGPGK1pG transcript because this mRNA has a shorter half-life and is therefore present at lower steady-state levels than the PGK1pG transcript in the *xrn1*Δ strain.

Similar fragments are also observed when cycloheximide is added to wild-type cells expressing the PGK1pG transcript (Fig. 9, lanes 4 and 5). In this case, the fragments are not very abundant at the 0-min time point because the block to 5′-to-3′ decay (cycloheximide) has just been applied. However, by 45 min, mRNAs corresponding to band B have accumulated to substantial amounts, and transcripts composing band C are detected. These species accumulated after transcription was blocked, indicating that they are derived from processing of the full-length 3′ end. The larger amount of band B relative to band C seen in this experiment compared with the other two conditions, in which 5′-to-3′ decay is inhibited continuously, is consistent with band B being an intermediate in the production of band C (24).

We interpret these results to indicate that the *PGK1* mRNA can be degraded from the 3′ end following deadenylation. Since the mRNA fragments generated by this decay mechanism are easily detected only when 5′-to-3′ exonucleolytic decay is blocked, this decay pathway is likely to be slower than 5′-to-3′ degradation. However, it should be noted that low levels of *PGK1* mRNA fragments shortened at the 3′ end can be detected even in wild-type cells (Fig. 9, lanes 6 and 7). This result suggests that some of the *PGK1* mRNA can normally be degraded from the 3′ direction following deadenylation (see Discussion).

DISCUSSION

The *PGK1* mRNA can be decapped and degraded 5′ to 3′ following deadenylation. Several lines of evidence indicate that at least some of the *PGK1* mRNA is decapped following deadenylation. First, following deadenylation in the *xrn1*Δ strain, we detected *PGK1* transcripts that were shortened at the 5′ end and lacked the 5′ cap structure (Fig. 2 to 4). The relatively low accumulation of these decapped species is consistent with our data indicating that there is a second pathway for the decay of the *PGK1* transcript (see below). A second line of evidence

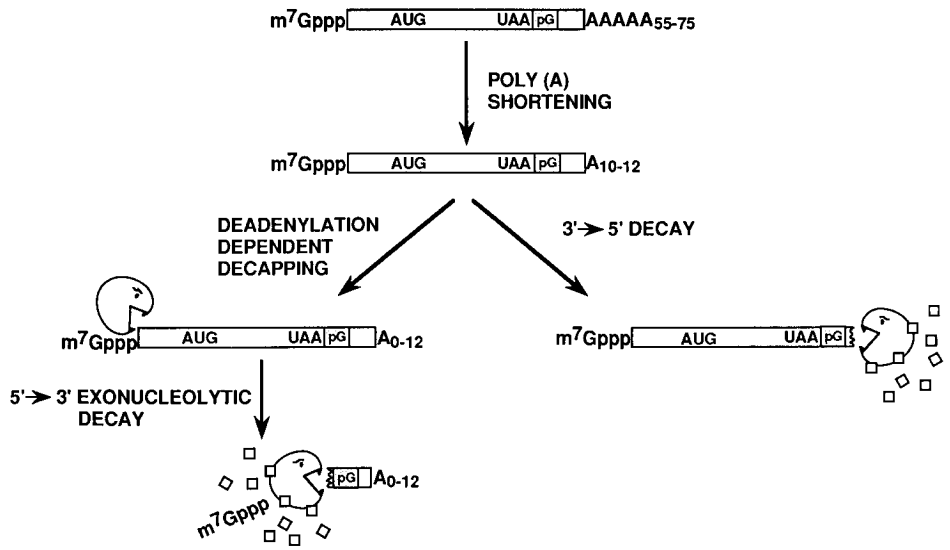

FIG. 10. Decay pathways of the *PGK1* mRNA. pG, poly(G) site.

showing that the *PGK1* mRNA is decapped following deadenylation comes from the analysis of *PGK1* transcripts containing poly(G) tracts in their 5′ UTRs. For these mRNAs, we observed that decay intermediates accumulated after deadenylation which were shortened at their 5′ ends to the 5′ side of the poly(G) tract (Fig. 5 and 6). When the pGPGK1pG mRNA was examined in the *xrn1*Δ strain, uncapped transcripts accumulated following deadenylation, with only small amounts of the decay products trimmed to the poly(G) tract being detected (Fig. 7). These results are consistent with the intermediates seen in wild-type cells being produced by decapping, followed by 5′-to-3′ degradation by Xrn1p. We conclude from the results of both approaches to inhibiting exonucleolytic decay that the *PGK1* mRNA can be decapped following deadenylation (Fig. 10). Since low levels of the decay intermediate trimmed to the 5′ side of the poly(G) insertion in the 3′ UTR (Fig. 1, 2, and 7) were detected in the *xrn1*Δ strain there are likely to be one or more additional 5′-to-3′ exonucleases that can substitute for Xrn1p.

The *PGK1* mRNA can be degraded 3′ to 5′ following deadenylation. Our data also suggest that the body of the *PGK1* mRNA can be degraded in a 3′-to-5′ direction following deadenylation (Fig. 10). This conclusion is based on the accumulation of mRNA fragments that are shortened at the 3′ end when the 5′-to-3′ degradation pathway is inhibited. Since these fragments are observed with three different blocks of 5′-to-3′ digestion, insertion of a 5′ poly(G) tract, addition of cycloheximide, or deletion of the *XRN1* gene, it is unlikely that they are artifacts of each independent experimental condition. Consistent with these fragments being produced by 3′-to-5′ degradation, they accumulate only when a poly(G) tract is present in the 3′ UTR to serve as a block to exonucleases. We interpret these observations to indicate that the *PGK1* mRNA can be slowly degraded from the 3′ end following deadenylation, although we cannot determine whether this 3′ decay process is exonucleolytic and/or endonucleolytic. Because these 3′-trimmed fragments can be observed at low levels in the wild-type strain without any block to the 5′-to-3′ exonucleolytic pathway (Fig. 9), we conclude that the *PGK1* mRNA can be degraded by at least two mechanisms following deadenylation. It is interesting that we do not see any evidence for 3′-to-5′ decay of the *MFA2* mRNA (22). This observation suggests that there may be mRNA-specific features which influence the susceptibility of a mRNA to this 3′-to-5′ decay process. The existence of a 3′-to-5′ decay pathway implies that this turnover mechanism may be preferred for some mRNAs.

Relative contribution of 5′-to-3′ and 3′-to-5′ degradation to the turnover of the *PGK1* mRNA. Since the *PGK1* mRNA can be degraded either 5′ to 3′ or 3′ to 5′ following deadenylation, an important issue is the relative contribution of each of these pathways to the overall turnover of the transcript. Although the relative importance of each pathway might vary under different conditions, in our experiments the 5′-to-3′ decay pathway is likely to be the primary mode of degradation. This conclusion is suggested by the observation that the fragments produced by 5′-to-3′ decay are easily detectable in wild-type cells, whereas fragments produced by 3′-to-5′ degradation are not observed at appreciable levels unless we first inhibit 5′-to-3′ decay (Fig. 8 and 9).

The relative importance of each pathway can also be crudely estimated from the ratio of the fragments produced by each pathway under steady-state conditions. It should be noted that this calculation requires several assumptions. First, it is assumed that the poly(G) structure is an equally efficient block to both the 5′-to-3′ and 3′-to-5′ degradative processes. In addition, we assume that the mRNA fragments produced by each pathway are substrates for the alternative pathway, and that the alternative pathway is the mechanism by which these fragments are ultimately degraded. For example, the mRNA fragment arising by 5′-to-3′ degradation to a poly(G) tract in the 3′ UTR is assumed to have the same rate constant for 3′-to-5′ digestion as the deadenylated full-length mRNA and to be ultimately degraded by this 3′-to-5′ pathway. In this case the flux of the mRNA fragment arising by 5′ to 3′ degradation {d[frag(5′→3′)]} can be expressed as

$$\frac{\mathrm{d[frag(5'\rightarrow 3')]}}{\mathrm{dT}} = k_{5'\rightarrow 3'}[\text{full-length(oligoA)}] - k_{3'\rightarrow 5'}[\mathrm{frag(5'\rightarrow 3')}]$$

In this equation, $k_{5'\rightarrow 3'}$ represents the rate constant for the

entire process of 5′-to-3′ decay, including decapping and 5′-to-3′ exonucleolytic digestion, and $k_{3'\rightarrow 5'}$ represents the rate constant for the process of 3′-to-5′ digestion. Rather than the concentration of the entire population of full-length mRNAs, the concentration of the deadenylated, full-length mRNA ([full-length(oligoA)]) is used in the equation because deadenylation is a prerequisite for 5′-to-3′ decay.

Similarly, the flux of the mRNA fragment arising by 3′-to-5′ degradation can be expressed as:

$$\frac{\mathrm{d}[\mathrm{frag}(3'\rightarrow 5')]}{\mathrm{dT}} = k_{3'\rightarrow 5'}[\text{full-length(oligoA)}] - k_{5'\rightarrow 3'}[\mathrm{frag}(3'\rightarrow 5')]$$

Since under steady-state conditions both of these equations are equal to zero, the equations can be equated and rearranged to yield the following expression for the ratio of the rate constants for 5′-to-3′ and 3′-to-5′ degradation:

$$\frac{k_{5'\rightarrow 3'}}{k_{3'\rightarrow 5'}} = \frac{\{[\text{full-length(oligoA)}] + [\mathrm{frag}(5'\rightarrow 3')]\}}{\{[\text{full-length(oligoA)}] + [\mathrm{frag}(3'\rightarrow 5')]\}}$$

Measurement of the relative concentrations on acrylamide Northern gels of each of these species under steady-state conditions indicates that [full-length(oligoA)] and [frag(5′→3′)] are roughly equal, with [frag(3′→5′)] being at most 1/20 of that level (data not shown). Insertion of these numbers into the equation presented above leads to the approximation that the 5′-to-3′ pathway of decay is faster than 3′-to-5′ decay by roughly a factor of 2. On the basis of this calculation, we suggest that the *PGK1* mRNA is degraded by both 5′-to-3′ and 3′-to-5′ processes after deadenylation, with the 5′-to-3′ process being the faster, and therefore primary, pathway in our experiments.

The effects of the *xrn1*Δ deletion on the turnover of the *PGK1* mRNA are consistent with this transcript decaying by a multistep pathway containing a branch point (Fig. 10). First, with the loss of Xrn1p, we would expect to reduce the amount of mRNA fragment trimmed from the 5′ end in to the poly(G) structure. This reduction in fragment levels is observed in Fig. 1, dropping from 30% of the full-length mRNA in the wild-type strain to barely detectable levels in the *xrn1*Δ strain. Moreover, as predicted from the branched pathway, inhibiting the 5′-to-3′ process by deletion of Xrn1p resulted in a corresponding increase in fragment levels arising by 3′-to-5′ decay (Fig. 8 and 9).

The loss of Xrn1p also led to the accumulation of a full-length, decapped intermediate. If the *xrn1*Δ was as effective at blocking 5′-to-3′ decay as the poly(G) tract, then the accumulation of this decapped species should be similar to the accumulation of fragments stabilized by the insertion of a poly(G) tract in the wild-type strain. Under steady-state conditions, the level of the mRNA fragment stabilized with a poly(G) tract in the 3′ UTR is approximately 30% of the level of the full-length transcript (Fig. 1). In comparison, the decapped species is present at a slightly lower level (approximately 20% of the full-length mRNA level) (Fig. 4). In the transcriptional pulse-chase experiments, there was also slightly less decapped species present in the *xrn1*Δ strain than the poly(G)-stabilized intermediates in wild-type cells (compare Fig. 2B and C). There are several possible explanations for the slightly lower level of decapped species. First, the poly(G) tract is probably a more effective block to 5′ digestion than the *xrn1*Δ mutation, since it is likely that there are other 5′-to-3′ exonucleases (22, 24). In addition, if the decapping enzyme interacts with Xrn1p, then loss of Xrn1p might decrease the rate of decapping. Another possibility is that some of the 5′-to-3′ trimmed fragments are generated by Xrn1p digestion after internal endonucleolytic cleavages instead of decapping.

One result was that the *xrn1*Δ mutation did not significantly affect the half-life of the *PGK1* mRNA. To predict the effect on half-life of the *xrn1*Δ mutation, we have computationally modeled the turnover pathway of the *PGK1* mRNA. Assuming that the 5′-to-3′ decay pathway is 2-fold faster than the 3′-to-5′ decay pathway, we calculate that a complete block to 5′ digestion would increase the half-life of the *PGK1* transcript by only approximately 1.7-fold (26a). This small predicted change in the half-life is due to the slow rate of deadenylation of the *PGK1* transcript and the alternative 3′-to-5′ decay pathway. There are several possible explanations for why the observed half-life is not altered even by this small amount. First, we could have underestimated the rate of the 3′-to-5′ pathway of decay. Second, decapping of the *PGK1* transcript might accelerate other non-*XRN1*-mediated decay processes, such as other 5′-to-3′ exonucleases or perhaps even the 3′-to-5′ decay pathway. Finally, there may be additional, uncharacterized mechanisms by which the *PGK1* mRNA can be degraded, perhaps including endonucleolytic cleavage. Any of these possibilities, alone or together, could easily account for the lack of any observed increase in the half-life of the *PGK1* mRNA in the *xrn1*Δ strain.

Previous experiments using the *PGK1* mRNA containing similar poly(G) insertions led to the suggestion that the *PGK1* mRNA was cleaved endonucleolytically within the coding region following deadenylation of the *PGK1* mRNA, thus producing a substrate for 5′-to-3′ degradation (34). The evidence for this cleavage event was the identification of an approximately 1.3-kb mRNA fragment on agarose Northern gels from a *PGK1* transcript containing poly(G) tracts in both the 5′ and 3′ UTRs. Mapping the 3′ ends of this fragment by S1 analysis with a probe whose 3′ end extended to the 3′ end of the poly(G) tract in the 3′ UTR detected mRNA ends within the coding region and led to the suggestion that the *PGK1* mRNA is endonucleolytically cleaved. Although we detect a similar 1.3-kb band in our experiments, our mapping of the 3′ end by Northern gel analysis (Fig. 9) and by RNase protection analysis using a probe that extends beyond the 3′ end of the mRNA (data not shown) positions the 3′ ends of this fragment 3′ of the poly(G) tract in the 3′ UTR. Moreover, since blocking the 5′-to-3′ pathway led to the accumulation of mRNA fragments shortened only at their 3′ ends, any endonucleolytic cleavage is likely to be slower than both pathways discussed above. However, it should be noted that detection of the cleavage products within the coding region required significant overexpression of the *PGK1* mRNA (34), which did not occur in our experiments. Therefore, although our results suggest that the predominant pathways of decay for the *PGK1* transcript are 5′ to 3′ or 3′ to 5′, it is possible that if both of these decay pathways are blocked, the *PGK1* mRNA can be cleaved internally.

Generality of deadenylation and decapping in the turnover of eukaryotic mRNAs. In combination with our previous work on the *MFA2* transcript (22), the experiments presented here indicate that both stable and unstable mRNAs in *S. cerevisiae* can be degraded by a mechanism in which deadenylation leads to decapping followed by 5′-to-3′ exonucleolytic degradation. Since decapping is dependent on prior poly(A) tail shortening, the decay rate of an mRNA is a function of its rates of deadenylation and decapping. Therefore, in this decay pathway, the decay rates of individual mRNAs are specified by differences in deadenylation rate (10, 23) and/or decapping rate, assuming that 5′-to-3′ exonucleolytic degradation is normally much faster than both deadenylation and decapping. For example,

the *PGK1* mRNA is stable because this transcript has a slow rate of deadenylation and a slow rate of decapping. In contrast, the *MFA2* mRNA is unstable because it exhibits rapid deadenylation and decapping. Thus, the control of decapping rate, by *cis*- and *trans*-acting features, will play a major role in determining differences in mRNA decay rates. An additional level of complexity arises for transcripts such as the *PGK1* mRNA that are also subject to 3′-to-5′ degradation and/or endonucleolytic cleavage. However, since several mRNAs examined in *xrn1*Δ strains accumulate under steady-state conditions as poly(A)-deficient molecules lacking the 5′ cap structure (15), it is extremely likely that the deadenylation/decapping pathway is a primary mode of degradation for many yeast transcripts. Moreover, since the poly(A) tail and the cap structure are found on essentially all mRNAs, this pathway could be a general mechanism for mRNA turnover in many eukaryotic cells (see also references 11 and 22).

Translation and mRNA turnover. One interesting result obtained from the experiments presented here was that the insertion of either the poly(G) tract or a strong stem-loop structure into the 5′ UTR, which inhibited translation, increased the deadenylation and decapping rates of the *PGK1* mRNA (Fig. 5). The rapid degradation of these transcripts is clearly mechanistically different from the extremely rapid decay triggered by premature termination of translation, which occurs independently of deadenylation (24). We interpret these observations to indicate that translation of the *PGK1* mRNA is required for its normally slow rates of deadenylation and decapping.

There are several possible explanations for how translation could affect deadenylation and decapping. Translation could slow decay by affecting the function of translation-dependent stability elements (14, 28) or by changing the subcellular location of the mRNA and thereby changing its susceptibility to degradation factors (21, 40). One appealing model is based on the observation that decapping requires prior deadenylation, suggesting an interaction, either direct or indirect, between the 5′ cap structure and the 3′ poly(A) tail (22). Interactions between the termini have also been proposed on the basis of the effects of the poly(A) tail (26) and 3′ UTR sequences on translation initiation (reviewed in reference 16) and on the presence of circular polysomes in electron micrographs (e.g., reference 6). We hypothesize that the rate of deadenylation and decapping is dependent on the state of this 5′-to-3′ interaction, which in turn is influenced by the process of translation (3, 22, 24). In this model, the increased rate of deadenylation and decapping seen for the untranslatable *PGK1* mRNAs, and the deadenylation-independent decapping triggered by early nonsense codons (24), would be due to alterations to the 5′-to-3′ interaction resulting from aberrant translation.

ACKNOWLEDGMENTS

We thank Hendrik Raué and the members of R.P.'s laboratory, especially Lianna Hatfield and Giordano Caponigro, for helpful comments on the manuscript.

This work was supported by the Howard Hughes Medical Institute, a grant to R.P. from the National Institutes of Health (GM45443), and a fellowship to C.J.D. from the Damon Runyon-Walter Winchell Cancer Research Fund (DRG-1141).

REFERENCES

1. **Aharon, T., and R. J. Schneider.** 1993. Selective destabilization of short-lived mRNAs with the granulocyte-macrophage colony-stimulating factor AU-rich 3′ noncoding region is mediated by a cotranslational mechanism. Mol. Cell. Biol. **13:**1971–1980.
2. **Amberg, D. C., A. L. Goldstein, and C. N. Cole.** 1992. Isolation and characterization of *RAT1*: an essential gene of Saccharomyces cerevisiae required for the efficient nucleocytoplasmic trafficking of mRNA. Genes Dev. **6:**1173–1189.
3. **Beelman, C. A., and R. Parker.** 1994. Differential effects of translational inhibition in cis and in trans on the decay of the unstable yeast *MFA2* mRNA. J. Biol. Chem. **269:**9687–9692.
4. **Brewer, G., and J. Ross.** 1988. Poly(A) shortening and degradation of the 3′ A+U-rich sequences of human c-*myc* mRNA in a cell free system. Mol. Cell. Biol. **8:**1697–1708.
5. **Caponigro, G., D. Muhlrad, and R. Parker.** 1993. A small segment of the *MAT*α*1* transcript promotes mRNA decay in yeast: a stimulatory role for rare codons. Mol. Cell. Biol. **13:**5141–5148.
6. **Christensen, A. K., L. E. Kahn, and C. M. Bourne.** 1987. Circular polysomes predominate on the rough endoplasmic reticulum of somatropes and mammotropes in the rat anterior pituitary. Am. J. Anat. **178:**1–10.
7. **Cigan, A. M., E. K. Pabich, and T. F. Donahue.** 1988. Mutational analysis of the *HIS4* translational initiator region in *Saccharomyces cerevisiae*. Mol. Cell. Biol. **8:**2964–2975.
8. **Cleveland, D.** 1989. Gene regulation through mRNA stability. Curr. Opin. Cell Biol. **1:**1148–1153.
9. **Coutts, M., and G. Brawerman.** 1993. A 5′ exoribonuclease from cytoplasmic extracts of mouse sarcoma 180 ascites cells. Biochim. Biophys. Acta **1173:** 57–62.
10. **Decker, C. J., and R. Parker.** 1993. A turnover pathway for both stable and unstable mRNAs in yeast: evidence for a requirement for deadenylation. Genes Dev. **7:**1632–1643.
11. **Decker, C. J., and R. Parker.** 1994. Mechanisms of mRNA turnover in eukaryotes. Trends Biochem. Sci. **19:**336–340.
12. **Elledge, S. E., and R. Davis.** A family of versatile centromeric vectors designed for use in the sectoring-shuffle mutagenesis assay in *Saccharomyces cerevisiae*. Gene **70:**303–312.
13. **Felici, F., G. Cesareni, and J. M. X. Hughes.** 1989. The most abundant small cytoplasmic RNA of *Saccharomyces cerevisiae* has an important function required for normal cell growth. Mol. Cell. Biol. **9:**3260–3268.
14. **Heaton, B., C. Decker, D. Muhlrad, J. Donahue, A. Jacobson, and R. Parker.** 1992. Analysis of chimeric mRNAs identifies two regions within the *STE3* mRNA which promote rapid mRNA decay. Nucleic Acids Res. **20:**5365–5373.
15. **Hsu, C. L., and A. Stevens.** 1993. Yeast cells lacking 5′ to 3′ exoribonuclease 1 contain mRNA species that are poly(A) deficient and partially lack the 5′ cap structure. Mol. Cell. Biol. **13:**4826–4835.
16. **Jackson, R. J., and N. Standart.** 1990. Do the poly(A) tail and the 3′ UTR control translation? Cell **62:**15–24.
17. **Kenna, M., A. Stevens, M. McCammon, and M. G. Douglas.** 1993. An essential yeast gene with homology to the exonuclease-encoding *XRN1*/*KEM1* gene also encodes a protein with exoribonuclease activity. Mol. Cell. Biol. **13:**341–350.
18. **Kozak, M.** 1991. Structural features in eukaryotic mRNAs that modulate the initiation of translation. J. Biol. Chem. **286:**19867–19870.
19. **Laird-Offringa, I. A., C. L. de Wit, P. Elfferich, and A. J. van der Eb.** 1990. Poly(A) tail shortening is the translation-dependent step in c-*myc* mRNA degradation. Mol. Cell. Biol. **10:**6132–6140.
20. **Larimer, F. W., and A. Stevens.** 1990. Disruption of the gene *XRN1*, coding for a 5 to 3′ exoribonuclease, restricts yeast cell growth. Gene **95:**85–90.
21. **Mason, J. O., G. T. Williams, and M. S. Neuberger.** 1988. The half-life of immunoglobulin mRNA increases during B-cell differentiation: a possible role for targeting to membrane-bound polysomes. Genes Dev. **2:**1003–1011.
22. **Muhlrad, D., C. J. Decker, and R. Parker.** 1994. Deadenylation of the unstable mRNA encoded by the yeast *MFA2* gene leads to decapping followed by 5′ to 3′ digestion of the transcript. Genes Dev. **8:**855–866.
23. **Muhlrad, D., and R. Parker.** 1992. Mutations affecting stability and deadenylation of the yeast *MFA2* transcript. Genes Dev. **6:**2100–2111.
24. **Muhlrad, D., and R. Parker.** 1994. Premature translational termination triggers mRNA decapping. Nature (London) **340:**578–581.
25. **Munns, T. W., M. K. Liszewski, J. T. Tellam, H. F. Sims, and R. E. Rhoads.** 1982. Antibody-nucleic acid complexes. Immunospecific retention of globin messenger ribonucleic acid with antibodies specific for 7-methyl guanosine. Biochemistry **21:**2922–2928.
26. **Munroe, D., and A. Jacobson.** 1990. mRNA poly(A) tail, a 3′ enhancer of translational initiation. Mol. Cell. Biol. **10:**3441–3455.

26a. **Parker, R.** Unpublished observation.

27. **Peltz, S. W., G. Brewer, P. Berstein, P. Hart, and J. Ross.** 1991. Regulation of mRNA turnover in eukaryotic cells. Crit. Rev. Eukaryotic Gene Expr. **1(2):**99–126.
28. **Peltz, S. W., A. H. Brown, and A. Jacobson.** 1993. mRNA destabilization triggered by premature translational termination depends on at least three cis-acting sequence elements and one trans-acting factor. Genes Dev. **7:**1737–1754.
29. **Sachs, A. B.** 1993. Messenger RNA degradation in eukaryotes. Cell **74:**413–421.
30. **Savant-Bhonsale, S. S., and D. W. Cleveland.** 1992. Evidence for instability of mRNAs containing AUUUA motifs mediated through translation-dependent assembly of a >20s degradation complex. Genes Dev. **6:**1927–1939.

31. **Shyu, A.-B., J. G. Belasco, and M. E. Greenberg.** 1991. Two distinct destabilizing elements in the c-fos message trigger deadenylation as a first step in rapid mRNA decay. Genes Dev. **5:**221–234.
31a. **Stevens, A.** Personal communication.
32. **Swartwout, S. G., and A. J. Kinniburgh.** 1989. c-*myc* mRNA degradation in growing and differentiating cells: possible alternative pathways. Mol. Cell. Biol. **9:**288–295.
33. **Vega-Laso, M. R. V., D. Zhu, F. Sagliocco, A. J. P. Brown, M. F. Tuite, and J. E. G. McCarthy.** 1993. Inhibition of translational initiation in the yeast *Saccharomyces cerevisiae* as a function of the stability and position of hairpin structures in the mRNA leader. J. Biol. Chem. **268:**6453–6462.
34. **Vreken, P., and H. A. Raué.** 1992. The rate-limiting step in yeast *PGK1* mRNA degradation is an endonucleolytic cleavage in the 3′-terminal part of the coding region. Mol. Cell. Biol. **12:**2986–2996.
35. **Williamson, J. R., M. K. Ragharaman, and T. R. Cech.** 1989. Monovalent cation-induced structure of telomeric DNA: the G-quartet model. Cell **59:** 871–880.
36. **Wilson, T., and R. Triesman.** 1988. Removal of poly(A) and consequent degradation of the c-fos mRNA facilitated by 3′ AU-rich sequences. Nature (London) **336:**396–399.
37. **Wisdom, R., and W. Lee.** 1990. Translation of c-myc mRNA is required for its post-transcriptional regulation during myogenesis. J. Biol. Chem. **265:** 19015–19021.
38. **Wisdom, R., and W. Lee.** 1991. The protein-coding region of c-myc mRNA contains a sequence that specifies rapid mRNA turnover and induction by protein synthesis inhibitors. Genes Dev. **5:**232–243.
39. **Yang, H., M. L. Moss, E. Lund, and J. E. Dahlberg.** 1992. Nuclear processing of the 3′-terminal nucleotides of pre-U1 RNA in *Xenopus laevis* oocytes. Mol. Cell. Biol. **12:**1553–1560.
40. **Zambetti, G., W. Schmidt, G. Stein, and J. Stein.** 1985. Subcellular localization of histone messenger RNAs on cytoskeleton-associated free polysomes in HeLa S3 cells. J. Cell Physiol. **125:**343–353.
41. **Zimmerman, S. B., G. H. Cohen, and D. R. Davies.** 1975. X-ray fiber diffraction and model-building study of polyguanylic acid and polyinosinic acid. J. Mol. Biol. **92:**181–192.